

Electron Phonon Superconductivity in LaNiOP

Alaska Subedi

*Department of Physics and Astronomy, University of Tennessee, Knoxville, Tennessee 37996-1200, USA and
Materials Science and Technology Division, Oak Ridge National Laboratory, Oak Ridge, Tennessee 37831-6114*

D.J. Singh and M.-H. Du

Materials Science and Technology Division, Oak Ridge National Laboratory, Oak Ridge, Tennessee 37831-6114

(Dated: October 29, 2018)

We report first principles calculations of the electronic structure, phonon dispersions and electron phonon coupling of LaNiPO. These calculations show that this material can be explained as a conventional electron phonon superconductor in contrast to the FeAs based high temperature superconductors.

PACS numbers: 74.25.Jb, 74.25.Kc, 74.70.Dd, 71.18.+y

The discovery of high temperature superconductivity in a series of FeAs based compounds, prototype LaFeAs(O,F) by Kamihara and co-workers¹ has led to intense investigation of these phases and the discovery of a number of new phases with critical temperatures in some cases near and above 55K.^{2,3,4} In addition, recently, high temperature superconductivity with similar properties has been found in simpler compounds based on FeAs sheets such as ThCr₂Si₂ structure type (Ba,K)Fe₂As₂.^{5,6} These Fe-based materials are commonly viewed as unconventional (non-electron-phonon) superconductors based on the high values of T_c , the proximity to magnetism and the fact that calculations of the electron phonon coupling show that it is far too weak to account for the superconductivity.^{7,8} It should be emphasized that these are rich structure types and that there is no doubt much compositional space that remains to be explored.^{9,10}

In this regard, besides the FeAs based phases, superconductivity is also observed in Ni based materials, including LaNiPO,^{11,12} pure, fluorine or Sr doped LaNiAsO,^{13,14,15} and LaNiBiO.¹⁶ Interestingly, both Ni and Fe are ambient temperature elemental ferromagnets, and many Fe and Ni compounds show magnetism. In addition, it is interesting to note a possible connection to the cuprates. Specifically, the Ni compounds are based on square lattices of nominally Ni²⁺ and superconduct with various dopings, including electron doping to yield a nominal d occupancy $8+\delta$, while the high T_c superconductors are based on square lattices of Cu²⁺ with hole doping for nominal d occupancy $9-\delta$, where δ is the doping level.

Returning to the connection with the Fe-based compounds, both electronic structure calculations^{17,18,19,20} and experiment show important differences between the Ni-based and Fe-based superconductors. In particular, the Fe-based materials show low carrier density with relatively small Fermi surfaces, high density of states and proximity to magnetism,^{8,17,21,22} while the Ni compounds show large Fermi surfaces, lower density of states and are apparently further from magnetic instabilities. This suggests that the Ni-based compounds may be a different class of superconductors, perhaps, considering the lower

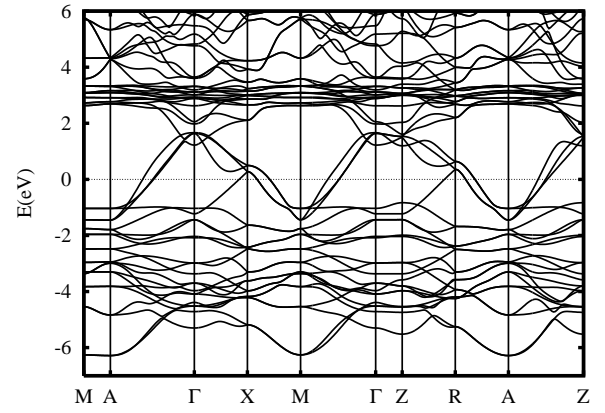


FIG. 1: Calculated LDA band structure of LaNiPO using the experimental lattice parameter and relaxed internal coordinates, $z_{\text{La}}=0.1506$ and $z_{\text{P}}=0.6210$.

T_c observed so far in this group, conventional electron-phonon materials. On the other hand, it may be noted that the kinds of measurements and calculations done so far would have given qualitatively similar results for cuprate superconductors in the optimal and overdoped regions - i.e. moderate density of states, high carrier density metals, apparently far from magnetism.

Here we report details of our previous electronic structure calculations as well as calculations of the phonon dispersions and electron-phonon coupling for LaNiPO. The calculations show that unlike the Fe-based materials, superconductivity in this Ni-based compound is readily explained by the standard electron-phonon mechanism. This means that the superconductivity of LaNiPO is not related to that of the FeAs based materials.

Our electronic structure was discussed briefly previously¹⁷ and is similar to that reported by Zhang and co-workers for the same compound.¹⁸ It also shows similarities to the electronic structures found for the other Ni-based compounds.^{19,20} Our electronic structure calculations were performed within the local density approximation (LDA) using the general potential lin-

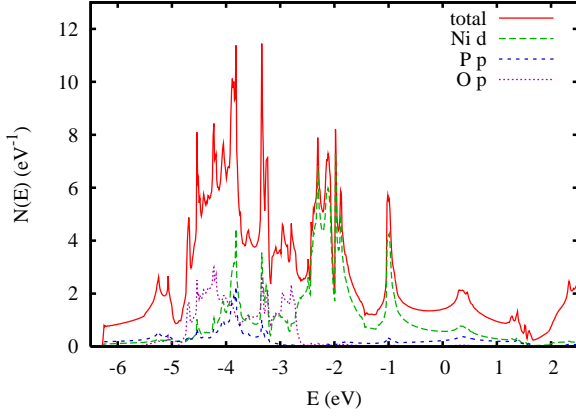


FIG. 2: (color online) Calculated LDA density of states of LaNiPO on a per formula unit both spins basis. The projections are onto the LAPW spheres.

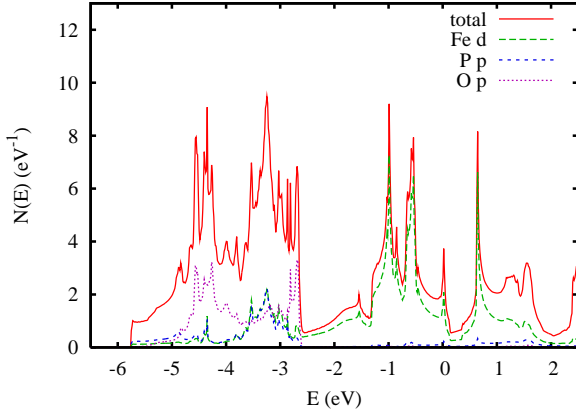


FIG. 3: (color online) Calculated LDA density of states of LaFePO on a per formula unit both spins basis. The projections are onto the LAPW spheres. The Fe sphere radius was $2.1 a_0$, which is equal to the Ni sphere radius used in Fig. 2.

earized augmented planewave (LAPW) method²³ as for LaFeAsO (Ref. 17). LAPW sphere radii of $2.2 a_0$, $2.1 a_0$, $2.1 a_0$ and $1.6 a_0$ were used for La, Ni, P, and O, respectively. In particular we used the experimentally reported tetragonal lattice parameters ($a=4.0461\text{\AA}$, $c=8.100\text{\AA}$)¹¹ and relaxed the internal coordinates which correspond to the La and P heights. We obtain $z_{\text{La}}=0.1506$ and $z_{\text{P}}=0.6210$, which are close to the reported experimental values of $z_{\text{La}}=0.1531$ and $z_{\text{P}}=0.6260$,¹¹ and $z_{\text{La}}=0.1519$ and $z_{\text{P}}=0.6257$.¹² This is different from the Fe-based compounds where pnictogen heights significantly lower than the reported experimental values are generally obtained.^{24,25}

The calculated band structure and electronic density of states (DOS) are shown in Figs. 1 and 2, respectively. The DOS for LaFePO, calculated in the same way is shown in Fig. 3 for comparison. The Fermi surface of LaNiPO is given in Fig. 4. As may be seen, these are very different in LaNiPO from those in LaFeAsO.

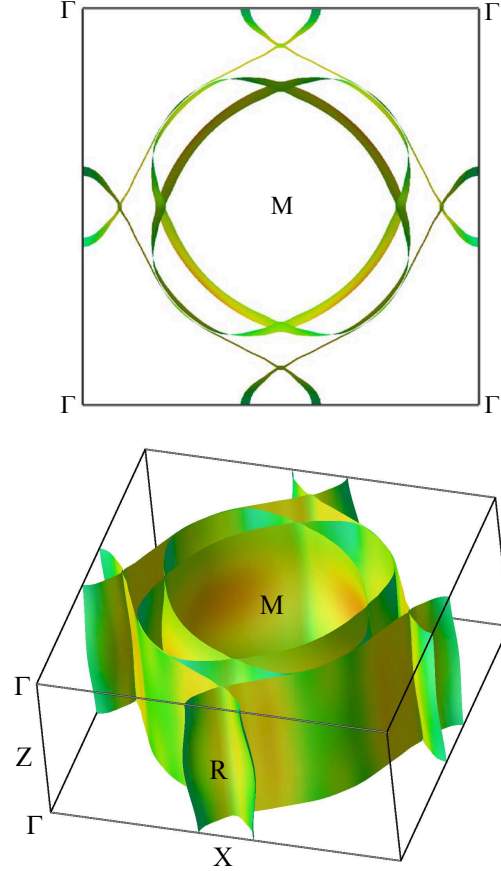


FIG. 4: (color online) Calculated LDA Fermi surface of LaNiPO shaded by velocity. The top panel shows a view along the tetragonal axis while the bottom panel shows a tilted view.

This is as might be expected from the different electron count. LaNiPO and LaFeAsO have a similar structure to the d bands, and in particular LaNiPO should be described as Ni^{2+} ions on a square lattice with direct hopping as well as a P induced crystal field. In fact, the projections of the density of states shows that there is a greater degree of covalency between Ni and P, than between Fe and As or Fe and P in the corresponding Fe-based materials. There remains a pseudogap at a d electron count of 6, however Ni^{2+} has 8 electrons. This places E_F well inside the upper manifold of d states. In this energy range the bands are derived from Ni d states hybridized with P p states. The bands at E_F are more dispersive than in the Fe compounds where E_F is lower. This leads to lower density of states with higher in plane Fermi velocity, $N(E_F)=1.41 \text{ eV}^{-1}$ per formula unit, $v_{xx}=3.75 \times 10^7 \text{ cm/s}$, $v_{zz}=0.39 \times 10^7 \text{ cm/s}$. The lower $N(E_F)$ puts the Ni based compound further from magnetism than the Fe-based materials, as was discussed.¹⁷ Furthermore, this compound is quite two dimensional in the sense that there is no 3D Fermi surface sheet. Based on the anisotropy of the Fermi velocity, the ratio of in-plane to c -axis conductivity for the Ni compound is ~ 100

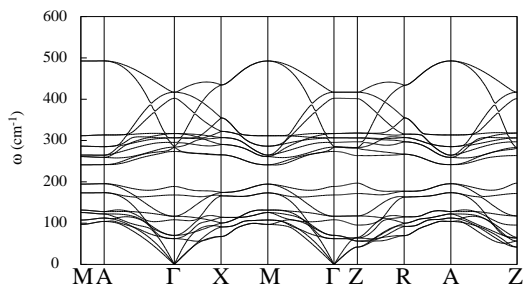


FIG. 5: Calculated phonon dispersions of LaNiPO as obtained within linear response.

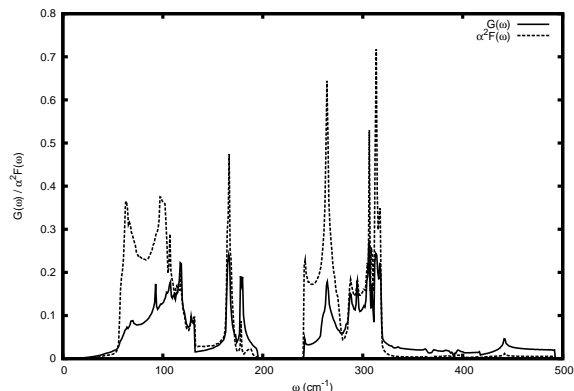


FIG. 6: Calculated phonon density of states and electron phonon spectral functional $\alpha^2F(\omega)$.

assuming isotropic scattering. The Fermi surface may be described as consisting of two large ellipsoidal cross-section electron cylinders around M, and a large hole section around Γ . This hole section intersects the zone boundary near X leading to an electron section around X.

The phonon and electron phonon calculations were performed in linear response, with the quantum espresso code²⁶ and ultrasoft pseudopotentials and the generalized gradient approximation of Perdew, Burke and Ernzerhof (PBE),²⁷ similar to our previous calculations for LaFeAsO.⁸ We did convergence tests for the basis set size, the planewave expansion of the charge density, the temperature broadening, and the Brillouin zone sampling. An 8x8x4 grid was used for the zone integration in the phonon calculations, while a more dense 32x32x8 grid was used for the zone integration in the electron-phonon coupling calculation. The basis set cut-off for the wavefunctions was 40 Ry, while a 400 Ry cut-off was used for

the charge density.

The calculated phonon dispersions of LaNiPO are shown in Fig. 5. The corresponding phonon density of states and Eliashberg spectral function $\alpha^2F(\omega)$ are shown in Fig. 6. The phonon dispersions show a set of 12 phonon bands extending up to $\sim 200 \text{ cm}^{-1}$, separated by a gap from 12 higher frequency bands extending up to $\sim 500 \text{ cm}^{-1}$ (note that there are 24 phonon branches since there are two formula units per primitive cell). The higher frequency manifold is derived mainly from O and P motions. Within this upper manifold the P contribution is mainly below $\sim 300 \text{ cm}^{-1}$, while the dispersive modes above 300 cm^{-1} are mainly O derived. The lower manifold from 0 to 200 cm^{-1} consists of the acoustic modes and modes of mixed, but mainly metal character.

We obtain a value of the electron phonon coupling $\lambda=0.58$ with logarithmically averaged frequency $\omega_{\text{ln}}=113 \text{ cm}^{-1}$. Relative to the phonon density of states, the spectral function is enhanced for the lower frequency metal modes, which have strong in-plane Ni character, and for the modes at the bottom of the upper manifold, which have strong P character. Thus in spite of the lower electronic density of states, we obtain stronger electron phonon coupling as compared with LaFeAsO, where $\lambda \sim 0.2$.^{7,8} Inserting these numbers into the simplified Allen-Dynes formula,

$$k_B T_c = \frac{\hbar \omega_{\text{ln}}}{1.2} \exp \left\{ -\frac{1.04(1+\lambda)}{\lambda - \mu^*(1+0.62\lambda)} \right\}, \quad (1)$$

with ordinary values of the Coulomb parameter μ^* yields values in reasonable accord with experiment. Specifically, for $\mu^*=0.12$ we obtain $T_c=2.6\text{K}$, which is in accord with the experimental value $T_c \sim 3\text{K}$,¹¹ or $T_c=4.2\text{K}$.¹²

In conclusion we find that LaNiPO has a conventional superconducting state which arises from band metal with moderate density of states and intermediate electron phonon coupling. This is in contrast to e.g. LaFeAs(O,F) which is a high density of states material, near magnetism, and with weak electron phonon coupling that can in no way explain the superconductivity. This leaving aside structure and chemistry, the superconductivity of LaNiPO and presumably the rest of the Ni-based oxypnictides is unrelated to that of the Fe-based materials.

We are grateful for discussions with I.I. Mazin, D.G. Mandrus, B.C. Sales, R. Jin, and M. Fornari and support from DOE, Division of Materials Sciences and Engineering.

¹ Y. Kamihara, T. Watanabe, M. Hirano, and H. Hosono, J. Am. Chem. Soc. **130**, 3296 (2008).

² Z.A. Ren, W. Lu, J. Yang, W. Yi, X.L. Shen, Z.C. Li, G.C. Che, X.L. Dong, L.L. Sun, F. Zhou, and Z.X. Zhao, Chinese Physics Letters **25**, 2215 (2008).

³ C. Wang, L. Li, S. Chi, Z. Zhu, Z. Ren, Y. Li, Y. Wang, X. Lin, Y. Luo, X. Xu, G. Cao and Z. Xi, arXiv:0804.4290 (2008).

⁴ H. Kito, H. Eisaki, and A. Iyo, J. Phys. Soc. Jpn. **77**, 063707 (2008).

- ⁵ M. Rotter, M. Tegel, D. Johrendt, I. Schellenberg, W. Hermes, and R. Pottgen, arXiv:0805.4021 (2008).
- ⁶ M. Rotter, M. Tegel, and D. Johrendt, arXiv:0805.4630 (2008).
- ⁷ L. Boeri, O.V. Dolgov, and A.A. Golubov, arXiv:0803.2703 (2008).
- ⁸ I.I. Mazin, D.J. Singh, M.D. Johannes, and M.H. Du, arXiv:0803.2740 (2008).
- ⁹ P. Quebe, L.J. Terbuchte, and W. Jeitschko, J. Alloys Compds. **302**, 70 (2000), and refs. therein.
- ¹⁰ M. Pfisterer and G. Nagorsen, Z. Nat. B **35**, 703 (1980).
- ¹¹ T. Watanabe, H. Yanagi, T. Kamiya, Y. Kamihara, H. Hiramatsu, M. Hirano, and H. Hosono, Inorg. Chem. **46**, 7719 (2007).
- ¹² M. Tegel, D. Bichler, and D. Johrendt, Solid State Sciences **10**, 193 (2008).
- ¹³ Z. Li, G.F. Chen, J. Dong, G. Li, W.Z. Hu, J. Zhou, D. Wu, S.K. Su, P. Zheng, N.L. Wang, and J.L. Luo, arXiv:0803.2572 (2008).
- ¹⁴ L. Fang, H. Yang, P. Cheng, X. Zhu, G. Mu, and H.H. Wen, arXiv:0803.3978 (2008).
- ¹⁵ G.F. Chen, Z. Li, D. Wu, J. Dong, G. Li, W.Z. Hu, P. Zheng, J.L. Luo, and N.L. Wang, arXiv:0803.4384 (2008).
- ¹⁶ V.L. Kozhevnikov, O.N. Leonidova, A.L. Ivanovskii, I.R. Shein, B.N. Goshchitskii, and A.E. Karkin, arXiv:0804.4546 (2008).
- ¹⁷ D.J. Singh and M.H. Du, Phys. Rev. Lett. **100**, 237003 (2008).
- ¹⁸ W.B. Zhang, X.B. Xiao, W. Li, W.Y. Yu, N. Wang, and B.Y. Tang, arXiv:0804.1398 (2008).
- ¹⁹ I.R. Shein, V.L. Kozhevnikov, and A.L. Ivanovskii, arXiv:0804.4064 (2008).
- ²⁰ I.R. Shein, V.L. Kozhevnikov, and A.L. Ivanovskii, arXiv:0804.4670 (2008).
- ²¹ S. Ishibashi, K. Terakura, and H. Hosono, J. Phys. Soc. Jpn. **77**, 053709 (2008).
- ²² T. Yildirim, arXiv:0804.2252 (2008).
- ²³ D.J. Singh and L. Nordstrom, *Planewaves Pseudopotentials and the LAPW Method, 2nd Ed.* (Springer, Berlin, 2006).
- ²⁴ Z.P. Yin, S. Lebegue, M.J. Han, B. Neal, S.Y. Savrasov, and W.E. Pickett, arXiv:0804.3355 (2008).
- ²⁵ I.I. Mazin, M.D. Johannes, L. Boeri, K. Koepernik, and D.J. Singh, arXiv:0806.1869 (2008).
- ²⁶ S. Baroni, A. dal Corso, S. de Gironcoli, P. Giannozzi, C. Cavazzoni, G. Ballabio, S. Scandolo, G. Chiarotti, P. Focher, A. Pasquarello, et al., <http://www.quantum-espresso.org>.
- ²⁷ J.P. Perdew, K. Burke, and M. Ernzerhof, Phys. Rev. Lett. **77**, 3865 (1996).